LBL-19888
Preprint

Lawrence Berkeley Laboratory
UNIVERSITY OF CALIFORNIA

RECEIVED
LAWRENCE
BERKELEY LABORATORY
DEC 4 1985
LIBRARY AND
DOCUMENTS SECTION

Submitted to Physical Review C

FAST AND SLOW PROCESSES IN THE FRAGMENTATION OF ^{238}U by 85 MeV/nucleon ^{12}C

K. Aleklett, W. Loveland, T. Lund, P.L. McGaughey,
Y. Morita, G.T. Seaborg, E. Hagebø, and I. Haldorsen

October 1985

TWO-WEEK LOAN COPY
This is a Library Circulating Copy
which may be borrowed for two weeks

NUCLEAR SCIENCE DIVISION

LBL-19888 c.2

Prepared for the U.S. Department of Energy under Contract DE-AC03-76SF00098

DISCLAIMER

This document was prepared as an account of work sponsored by the United States Government. While this document is believed to contain correct information, neither the United States Government nor any agency thereof, nor the Regents of the University of California, nor any of their employees, makes any warranty, express or implied, or assumes any legal responsibility for the accuracy, completeness, or usefulness of any information, apparatus, product, or process disclosed, or represents that its use would not infringe privately owned rights. Reference herein to any specific commercial product, process, or service by its trade name, trademark, manufacturer, or otherwise, does not necessarily constitute or imply its endorsement, recommendation, or favoring by the United States Government or any agency thereof, or the Regents of the University of California. The views and opinions of authors expressed herein do not necessarily state or reflect those of the United States Government or any agency thereof or the Regents of the University of California.

LBL-19888

Fast and Slow Processes in the Fragmentation of ^{238}U by 85 MeV/nucleon ^{12}C

K. Aleklett, W. Loveland, T. Lund, P.L. McGaughey,
Y. Morita, G.T. Seaborg, E. Hagebø, and I. Haldorsen

Lawrence Berkeley Laboratory
University of California
Berkeley, California 94720

October 1985

LBL-19888

Fast and slow processes in the fragmentation of ^{238}U by 85 MeV/nucleon ^{12}C

K. Aleklett
The Studsvik Science Research Laboratory S-61182 Nyköping, Sweden

W. Loveland
Oregon State University Corvallis, OR 97331

T. Lund
Philipps Universität D-3550 Marburg, Federal Republic of Germany

P. L. McGaughey,* Y. Morita†, G.T. Seaborg
Lawrence Berkeley Laboratory Berkeley, CA 94720

E. Hagebø, I Haldorsen
University of Oslo Oslo, Norway

ABSTRACT

Target fragment distributions were measured using radiochemical techniques for 48 different fragments ($28 \leq A \leq 185$) from the interaction of 85 MeV/nucleon ^{12}C with ^{238}U. The laboratory system angular distributions are forward peaked and generally flat beyond 90°. When compared to similar distributions from the 85 MeV/nucleon ^{12}C+ ^{197}Au reaction, the U target fragment distributions are less forward peaked, consistent with lower momentum transfer. The (A=80–120) fission fragment distributions were symmetric about 90° in the moving frame, indicative of a "slow" process in which statistical equilibrium has been established. The average fissioning system angular momentum was deduced to be 25–35hbar. The observation that the fragments with low N/Z showed more anisotropic distributions than fragments with high N/Z was accounted for in firestreak model calculations as being due to a single reaction mechanism with varying amounts of deposition energy. The lightest ($A<60$) and heaviest (A = 139–169) members of the central fission-like bump in the mass distribution had moving frame angular distributions that were asymmetric in the moving frame. Furthermore, the heavy fragment complement of the ^{46}Sc distribution was similar in shape to the ^{146}Gd distribution, suggesting these fragments were produced in a new intermediate energy reaction mechanism, a fast, non-equilibrium, very asymmetric fission of a heavy nucleus.

* Present Address: Los Alamos National Laboratory, Los Alamos, N.M.
† Present Address: UCSF, Radiologic Imagery Lab., S. San Francisco, CA 94080

This work was supported in part by the U. S. Department of Energy under contract DE-AC03-76SF00098 and DE-AM06-76RL02227, task agreement DE-AT06-76ER-70035, Mod. A009, the Swedish Natural Science Research Council, the BFMT (Bonn) and the Norwegian Research Council for Science and the Humanities.

I. INTRODUCTION

In recent years intermediate energy heavy ion reactions, i.e., reactions in which the projectile energy ranges from 10 to 200 MeV/nucleon, have been studied extensively. Such reactions are interesting because of (a) unusual phenomena predicted to occur in these reactions, such as nuclear liquid-gas phase transitions and (b) the possibility of observing the transition from nuclear reaction phenomena dominated by "mean-field" behavior ($E_{proj} \leq 10$ MeV/nucleon) to those reactions characterized by interactions between individual nucleons ($E_{proj} > 200$ MeV/nucleon). Experimental studies of these reactions have been aided by relatively recent accelerator developments at CERN, MSU and GANIL that have made available intense heavy ion beams in this energy region. The goal of many experimenters working with these reactions is to understand the mechanisms of the nuclear reactions that occur. In this report we shall present evidence concerning the time scale and character of some of these reaction mechanisms.

One of the simple observables of any nuclear reaction is the spatial distribution of the reaction products, i.e., the product angular distributions. One of the most important characteristics of a nuclear reaction is its time scale, i.e., how fast does it occur, how long does any intermediate (mono or di-nuclear) species formed in the reaction exist. This observable and this fundamental reaction characteristic are related, in that one can show that for any moderate or highly excited, long-lived, intermediate species the angular distribution of emitted particles (or break-up products) in the frame moving with the velocity of the intermediate species must be symmetric about a plane normal to the direction of motion of the intermediate system. By the term "long-lived" we mean that the intermediate species lives long enough that the statistical assumption concerning level densities is valid, i.e., a statistically large number of overlapping levels with randomly distributed phases is populated so that interferences between them will cancel. The time for this equilibration process to occur had been calculated[1] to be $<2\text{–}3 \times 10^{-23}$ sec. An example of the application of this idea is the study of fragmentation processes in high energy p-nucleus collisions in which the time scale of processes leading to fragments with $A_{frag} \leq 1/3\ A_{target}$ was shown to be "fast" by virtue of having asymmetric fragment angular distributions in the moving frame.[2] In addition to this fundamental relationship of the fragment angular distributions and a gross measure of the time scale of the reaction, the angular distributions are also useful in defining certain features of the reaction mechanisms. With these ideas in mind, we report herein the results of measuring the angular distributions of 48 different target fragments in the interaction of intermediate energy (85 MeV/nucleon) ^{12}C with ^{238}U.

When this work is viewed in the context of relevant previous work certain studies stand out. The first of these is a study of the fragment angular distributions in the interaction of 85 MeV/nucleon ^{12}C with another high mass target, ^{197}Au.[3] In this work, we established that the angular distributions of light fragments ($A_{frag} < 60$) were asymmetric in the moving frame indicative of their production in a fast process without the establishment of statistical equilibrium. The fission fragments showed angular distributions that were symmetric in the moving frame. For the heaviest fragments ($A > 145$), which are mostly spallation products, the experimental evidence was not clear. It was not possible to find a moving frame in which the fragment distributions were symmetric about 90°, but for many cases the range of moving frame velocities included values that were so large as to cause ambiguous, double-valued results for the lab to moving frame transformation. In these cases the transformations could not be made and no definitive conclusion could be reached about the symmetry of the moving frame distributions.

For the reaction studied in this work the isobaric yields of the target fragments (Fig. 1) have been measured previously.[4] From examining this isobaric yield distribution, one concludes that there is a large probability for fission ($50 \leq A \leq 160$) with a much smaller probability for spallation-like events ($A \geq 200$). The fragments with $160 \leq A \leq 200$ appear to originate as either fission fragments or spallation products. Detailed alkali metal isotopic yields for this reaction have also been reported.[5] These distributions have been analyzed in terms of two components: a neutron-rich component attributed to low excitation energy peripheral reactions, and a neutron-deficient component attributed to more central collisions followed by fission and/or spallation. The average momentum transfer for all events leading to fission is 1.2 GeV/c [6] with the average momentum transfer for events that produce light fragments ($Z \leq 20$) being ~ 2.0 GeV/c.

In this work we use activation techniques to measure the target fragment angular distributions for the reaction of 85 MeV/nucleon ^{12}C with ^{238}U. Because of the good detection sensitivity of such techniques, we are able to measure complete (7–151°) angular distributions for many (48) different fragments including fragments with A>160, whose detection would be difficult using counter techniques. By using a ^{238}U target rather than the ^{197}Au target used in our previous work,[3] we are better able to study the effect of fragment N/Z upon the angular distributions. Furthermore, by comparison of these results with those obtained with a ^{197}Au target, we can identify some of the effects of target (Z,A) upon reaction mechanism.

For the reaction of 85 MeV/nucleon ^{12}C with ^{238}U, we observe the majority of fission events to be due to "slow" processes with symmetric angular distributions in the moving frame. For the light fragments (A<60) which may result from a very asymmetric "fission", we observe their production mechanism to be "fast", leading to asymmetric moving frame distributions. However, these distributions are far less forward peaked than those in the reaction of 85 MeV/nucleon ^{12}C with ^{197}Au, indicative of their production in events of lower momentum transfer. The variation of fission fragment angular distributions with fragment N/Z is smooth and continuous with the high N/Z fragments having less forward peaked distributions. The distinction between neutron-rich and neutron-deficient fragments, however, seems only to be due to differences in de-excitation mechanisms rather than reflecting any differences in primary formation processes. Finally, we find the angular distributions of the heaviest fission fragments (A>130) to be asymmetric in the moving frame, indicative of a fast non-equilibrium production mechanism. Some evidence is discussed that indicates these fragments may be the complements of the light fragments.

II. EXPERIMENTAL

The experimental methods used in this work to measure the fragment angular distributions were identical with those previously used[3] in the study of the reaction of 85 MeV/nucleon ^{12}C with ^{197}Au. (The two studies were actually performed concurrently.) An integral particle flux of ~ 6.7×10^{15} ions/936 min of 85 MeV/nucleon ^{12}C ions from the CERN SC synchrocyclotron was used in this study. The absolute magnitudes of the differential cross sections were determined by integrating them and normalizing the resulting fragment production cross sections to previously measured values.[4,5] As in the previous study, two thin U targets, one facing forward and one facing backward, consisting of evaporated deposits of UF_4 on a 13.4 mg/cm^2 Al backing, were used. The Al backing was sufficiently thick to stop any fragments from the "forward" target traveling backward and vice versa. The "forward" and "backward" ^{238}U deposit thicknesses were determined by α-counting to be 783 and 804 μg/cm^2, respectively. The catcher foil geometry was identical to that used previously except that the backward angle catchers subtending 143–153° and 153–166° were combined into a single catcher subtending 143–166°. The off-line γ-ray spectroscopy to identify the nuclides present in the catcher foils was carried out as described previously.[3] The reader is referred to Ref. 3 also for discussions of angular resolution and the influence of fragment scattering upon the results.

III. RESULTS

The laboratory frame angular distributions for the 48 target fragments measured in this work are tabulated in Table I in the form of absolute differential cross sections. To simplify the discussion of these results, we have selected a representative subset of these data for a detailed analysis. The measured angular distributions for the 14 members of this subset are shown in Figs. 2–5.

The "light" (A<60) fragment angular distributions are strongly forward-peaked with relatively constant differential cross sections at backward angles (Fig. 2). The fission fragment angular distributions are less forward-peaked than the light fragment distributions, and among themselves, have similar shapes. The degree of forward-peaking decreases with increasing fragment N/Z (Figs. 3–4). The angular distributions of the heaviest fragments are very strongly forward-peaked with the degree of forward peaking increasing as the fragment A increases (Fig. 5).

Each fragment angular distribution was integrated from 0 to $\pi/2$ and $\pi/2$ to π to obtain the ratio of fragments recoiling forward (F) from the target to those recoiling backward (B). To extract further information from the data, the laboratory-system angular distributions were transformed into the moving frame of the target residue following the initial projectile-nucleus encounter. To do this we have used the well known two step vector model in which it is assumed that the final velocity of the fragment in the laboratory system can be written as $v_{lab} = V + v$, where the velocity v is the velocity of the moving frame and V is the velocity kick given the target fragment by fission or particle emission at an angle θ_{MF} with respect to the beam direction in the moving frame. The vector v has components of $v_{parallel}$ and v_{perp} parallel and perpendicular to the beam direction. In lieu of detailed information about v_{perp}, the general strong forward-peaked nature of the distributions, and the difficulty of obtaining information about v_{perp}, we have assumed $v_{perp} = 0$. We have used standard formulas[7] to make laboratory to moving frame transformations for $d\sigma/d\Omega$ and θ. For the value of $\eta_{parallel}$ ($= v_{parallel}/V$) needed to make such transformations, we have used $\eta_{parallel}$ as derived from integrating our angular distributions, where $\eta_{parallel} = (F - B)/(F + B)$. The results of these transformations are shown in Figs. 6–9.

The moving frame angular distributions for the light fragments (Fig. 6) are asymmetric, indicative of their production in a "fast" process assuming, of course, that the laboratory to moving frame transformation has been carried out correctly (see Section IV for discussion). The fission fragment moving frame distributions (Fig. 7) are symmetric in the moving frame, characteristic of a "slow" reaction process, while the distributions for the heaviest fragments are grossly asymmetric in the moving frame (Fig. 8).

For those nuclides with symmetric moving frame distributions (such as those shown in Fig. 7), a conventional representation of the angular distributions in the moving frame is

$$W(\theta_{MF}) = \frac{1+(b/a)\cos^2\theta_{MF}}{1+b/3a} \quad . \tag{1}$$

It can be shown[8] that the laboratory system angular distribution can be expressed in terms of $\eta_{parallel}$ and b/a as:

$$F_L(\theta_L) = \frac{1 + (b/a)\cos^2[\,\theta_L + \sin^{-1}(\eta_{parallel}\sin\theta_L)]}{1 + b/3a} \times \frac{[\eta_{parallel}\cos\theta_L + (1 - \eta_{parallel}\sin^{-2}\theta_L)^{1/2}]^2}{(1 - \eta^2_{parallel}\sin^2\theta_L)^{1/2}} \tag{2}$$

Either equations (1) or (2) along with values of $\eta_{parallel}$ determined above were used to determine the "best fit" values of (b/a) for each nuclide (Table II). Typical fits to the data are shown in Fig. 7. The data are well represented by these formulas with b/a>0. (This finding reinforces a point made earlier[3] that the most popular version[9] of the two-step vector model used to analyze thick target-thick catcher recoil data is not appropriate for use in intermediate energy heavy ion reaction studies. This version assumes b/a=0. This assumption can lead to serious errors even for events in which the reaction has a "fast-slow" character.)

IV. DISCUSSION

A. Comparison with previous measurements

It is interesting to compare the shapes of the observed distributions with previous work. The angular distributions of the light fragments ^{46}Sc and ^{59}Fe from the interaction of 85 MeV/nucleon ^{12}C with ^{238}U (this work) and ^{197}Au (Ref. 3) are compared in Fig. 2. The U target fragment distributions are less forward-peaked than the Au target fragment distributions. A possible explanation for this observation concerns the mechanisms for the production of these fragments. In U target fragmentation, this group of fragments appears to be part of the low mass tail of the fission mass distribution (Fig. 1) suggesting a very asymmetric binary division of the

nucleus is involved in their production. For the fragmentation of ^{197}Au by 85 MeV/nucleon ^{12}C, the situation appears to be more complicated. The light fragments (A<60) do not appear to be part of the central fission related peak in the mass distribution[10] (Fig. 9) but are partly (or wholly) due to processes other than fission. Such "fragmentation" processes are known in higher energy reactions[11] to have energy thresholds that are much greater than the thresholds for fission. All of these arguments point to the need for a greater energy deposit in a Au nucleus to produce these light fragments which in turn would cause a mere forward-peaked distribution. Even if one were to argue that these fragments were produced by a very asymmetric fission of either Au or U, it has been shown[6] that the average momentum transfer leading to fission events in the less fissionable Au nucleus is 1.6 GeV/c compared to 1.2 GeV/c for U fission induced by 85 MeV/nucleon ^{12}C.

Our fragment angular distributions can be compared to similar ones observed in p-nucleus collisions. For example, one can note that the anisotropy ($0^\circ/90^\circ$) of the ^{133}Ba^m distribution in this work is 1.61 compared to anisotropies of 1.09 and 1.04 for ^{131}Ba and ^{135}Ba^m in the interaction[12] of 0.8 GeV p+^{238}U. (In comparing p-nucleus and nucleus-nucleus fragmentation for this projectile energy, it has been shown[5] that one should compare studies in which the total projectile kinetic energies are similar.) This observation is consistent with the observations[13] at higher energies in which it was found that in nucleus-nucleus collisions the momentum imparted to the target nucleus is far greater than that observed in p-nucleus collisions.

Thus we would conclude that insofar as such comparisons are possible, our observations are consistent with other observations of similar properties in p-nucleus and nucleus-nucleus collisions.

B. Comparison with firestreak model

One striking feature of the fission fragment distributions is the variation of the anisotropy with the fragment N/Z ratio (Fig. 4). The more n-deficient fragments have more strongly forward-peaked distributions. Assuming that the fission fragment kinetic energies vary relatively slowly with A for the Sb isotopes (i.e., as $\sim A^{-1/3}$), the data of Table II would indicate that the n-deficient species result from interactions with significantly greater linear momentum transfer than the n-rich species (greater η_{parallel}) and have more anisotropic moving frame distributions (greater b/a). We thought it would be interesting to see if a frequently used phenomenological model for target fragmentation, the nuclear firestreak model,[14] could predict the observed behavior. (The details of this model and its application to target fragmentation studies has been described elsewhere.[3,4]) In Fig. 3b we show the predicted angular distributions for ^{122}Sb and ^{128}Sb fragments from the interaction of 85 MeV/nucleon ^{12}C with ^{238}U. It is clear that the predicted distributions agree qualitatively, if not quantitatively, with the observed distributions. (Within the model, the differences in the angular distributions for n-rich and n-poor species arise strictly from the momentum transfer in the initial part of the reaction since the moving frame distributions are assumed to be isotropic.) If one takes the firestreak model predictions seriously in this case, then one concludes that both n-rich and n-poor fragments result from a single mechanism, fission, occurring after varying amounts of energy are deposited in the target nucleus in the initial projectile-target encounter. A similar conclusion has been reached[15] in evaluating the fission of ^{238}U induced by 0.7 GeV protons. While it is possible to analyze the isotopic distributions of fission fragments such as these in terms of separate n-rich and n-poor components[5], the meaning of such analyses is questionable in light of our findings.

C. Moving frame angular distributions

The moving frame angular distributions of the average fission fragments are symmetric about 90° and adequately represented by the simple form of equation (1) (Fig. 7). Thus the majority of these fragments result from conventional fission processes involving a "slow" step with the establishment of statistical equilibrium. Because such information will be valuable in examining the properties of the other members of the fission distribution, we attempted to extract some crude estimates of the angular momenta of these systems.

Huizenga *et al.*[16] have shown that the angular distribution of an excited fissioning system with angular momentum J (and projection on the beam axis M = 0) can be written as:

$$W^{J}_{M=0}(\theta) =$$

$$\frac{(\frac{1}{2}\pi)(2J+1)\exp\left[-(J+\frac{1}{2})^2\sin^2\theta/4K_0^2\right]}{2\pi\,(\frac{1}{2}\pi^{\frac{1}{2}})\,(2K_0^2)^{\frac{1}{2}}\mathrm{erf}\left[(J+\frac{1}{2})/(2K_0^2)^{\frac{1}{2}}\right]}$$

$$\times J_0\left[i(J+\tfrac{1}{2})^2\sin^2\theta/4K_0^2\right] \quad , \tag{3}$$

where J_0 is the zero-order Bessel function with an imaginary argument, and $\mathrm{erf}[(J+\frac{1}{2})/2K_0^2]$ is the error function defined by

$$\mathrm{erf}(x) = \left(\frac{2}{\pi^{\frac{1}{2}}}\right)\int_0^x \exp(-t^2)dt \quad . \tag{4}$$

K_0^2 is the mean-square projection of J upon the nuclear symmetry axis. For a Fermi gas K_0^2 is given as

$$K_0^2 = I_{rigid}T/\mathrm{hbar}^2 \quad , \tag{5}$$

where I_{rigid} is the rigid-body moment of inertia of the fissioning system and T is its temperature. To use eq. (3) to calculate the moving frame fission-fragment angular distribution, we would need to know the J and syntax error file -, between lines 578 and 578 E distributions for each fissioning system, K_0^2 for each system, and be assured that M=0 along with appropriate averages over all fissioning systems. None of these conditions are fulfilled in the present case. However, eq. (3) can be used, with certain assumptions to make a crude, "ball-park" estimate of the average angular momentum of the "average" fissioning system in the reaction under study. For example, this procedure can be applied to angular distribution data[17] for the complete fusion of 291 MeV ^{40}Ar with ^{238}U, where the temperature of the fissioning system is known, to deduce a value of the average J of the fissioning system that is in good agreement with the average J value deduced from the measured $\mathrm{scriptl}_{crit}$ for the system.

From firestreak model calculations, we can get an estimate of the excitation energy of the "average" fissioning nucleus of E^*345 MeV. Using the relations $E^*=aT^2-T$ and $I_{rigid}=\frac{2}{5}r_0^2A^{5/3}$ with r_0=1.25 fm and a=A/10, we can calculate $K_0^{2\sim}$ 529. Using eqs. (3–5) we fit the moving frame fission fragment angular distributions ($84 \leq A \leq 110$) to extract a best fit value of J, i.e., $\langle J\rangle$=25–35hbar. (The firestreak model predicts the "average" fissioning system angular momentum to be 27hbar, in good agreement with the deduced "ball-park" estimate.)

The moving frame angular distributions of the light (A<60) fragments and the heavy fragments ($A \geq 139$) are grossly asymmetric with respect to a plane normal to the beam axis (Figs. 6 and 8). This is indicative of production of these fragments in a "fast" process without the establishment of statistical equilibrium. We have searched over a wide range of $\eta_{parallel}$ values (O.1–O.99) and did not find any value that properly symmetrized any of these distributions.

Asymmetric moving frame distributions for the A<60 fragments were observed previously for the 85 MeV/nucleon ^{12}C+^{97}Au reaction. Lynen *et al.*[6] did show that for the C+Au reaction, these fragments were produced by a binary breakup mechanism. In Ref. 3, we showed that an "equilibrium" very asymmetric fission mechanism, first suggested by Moretto,[18] was not playing an important role in this reaction. We also searched for the heavy fragment complement of the light fragments, but due to the large yield of heavy fragments from spallation-like processes, we were unable to find any evidence for the existence of these complementary fragments from a binary breakup.

With a U target, however, the situation is potentially different. The target fragments that can clearly be identified with spallation-like processes appear to be restricted to $A \geq 200$. Thus we thought it might be interesting to search for the heavy fragment complement of ^{46}Sc. We show

(in Fig. 8) the general similarity between the ^{146}Gd moving frame distribution and the calculated distribution for the complementary fragment to ^{46}Sc. It would be indeed fortuitous in an experiment such as we have performed, to find among the half dozen or so heavy fragments whose angular distribution we have measured the exact kinematic complement of a light fragment distribution. Furthermore, a single-particle inclusive experiment such as this is not the best way to look for kinematic complementarity. Nonetheless, the similarity between the ^{146}Gd distribution and the calculated "^{46}Sc-complement" distribution is quite striking. Further support for this idea is seen in Fig. 1 where we show the A = 46 and A = 146 fragments to occupy approximately complementary positions in the fission-like portion of the mass yield curve.

Another parameter that should also be indicative of kinematic complementarity is $\eta_{parallel}$ ($=v_{parallel}/V$). The values of $\eta_{parallel}$ for ^{146}Gd and ^{46}Sc are O.64 and O.27, respectively. If ^{46}Sc and ^{146}Gd came from the same asymmetric fission event, we would expect $v_{parallel}$ to be the same for both fragments, with $V_{Gd} = \sqrt{\frac{46}{146}} V_{Sc}$. Thus if $\eta_{parallel} = 0.27$ for ^{46}Sc, we would expect $\eta_{parallel}$ for ^{146}Gd to be O.48 instead of O.64. But we also must be aware that $\eta_{parallel}$ is quite sensitive to modest changes in fragment N/Z. Thus we are somewhat reassured to note that $\eta_{parallel}$ for ^{149}Gd is O.51, is in reasonable agreement with that expected for the kinematic complement of ^{46}Sc. (Unfortunately the measured angular distribution for ^{149}Gd is not well enough defined to make the type of comparison made in Fig. 8 for ^{46}Sc and ^{146}Gd.) Therefore, we conclude that due to: a) the apparent complementarity of A~ 46 and A~ 146 in the mass-yield curve, b) the similarity between the shapes of the ^{146}Gd moving frame distribution and that of the heavy fragment complement of ^{46}Sc, and c) the fact that the $\eta_{parallel}$ values for ^{46}Sc and ^{149}Gd are consistent with complementarity, it is plausible (but not proven) that these fragments are kinematic complements.

Thus it becomes interesting to speculate that we may have observed a new intermediate energy heavy ion reaction mechanism, a "fast" non-equilibrium very asymmetric fission. (The actual process could very well be characterized by a very broad symmetric mass distribution that is "hidden" under the more abundant average fission distribution and only becomes visible to us in the low and high mass tails of the distribution.)

Two fission processes with "fast" characteristics have been noted as occurring in different energy regimes. At lower projectile energies, a number of observers have reported a significant increase in the width of the fission mass distribution when the angular momentum of the projectile-target composite system exceeds the rotating liquid drop model limit, i.e., when the fission barrier becomes zero due to angular momentum. Current theories[19] of this "fast fission" process point to a system where the total interaction potential has a pocket ($Z1 \cdot Z2 < 2500$–3000) and $\text{scriptl}_{B_f} \leq \text{scriptl} \leq \text{scriptl}_{crit}$ where scriptl_{crit} is the critical angular momentum for fusion. While the first condition ($Z_1 \cdot Z_2 < 2500$) is satisfied in the reaction under study, the second is not,[20] in that $\text{scriptl}_{crit} = 61\text{hbar}$ while $\text{scriptl}_{B_f} = 78\text{hbar}$. Thus there are no "bound" partial waves that exceed scriptl_{B_f}.

If A~ 46 and A~ 146 fragments are complementary fragments, then a large amount of mass has been "lost" from the system in the fission process without disturbing the two body kinematics. Similar types of "fast" fission processes with large mass loss prior to fission and broad mass distributions have been observed in high energy p-nucleus collisions[21,22]. In these events the fission fragment kinetic energies were observed to be larger than those expected for fission. But these fragments were also observed to have large transverse momentum and be preferentially emitted at 90° to the beam axis, a condition not observed in our studies.

Thus we conclude that our results are suggestive of a new intermediate energy reaction process, a fast, non-equilibrium, binary division of the nucleus unlike processes seen at lower or higher projectile energies. The process is apparently accompanied by a large mass loss. Since the interaction potential has pockets for partial waves up to scriptl = 61 and the average fission event involves lower partial waves (based on the previous estimate of the mean J of the fissioning system), one is further tempted to associate this process with the higher "bound" partial waves.

V. SUMMARY

What have we learned about target fragmentation in the interaction of 85 MeV/nucleon ^{12}C with ^{238}U from this work and that of others? Most target-projectile interactions result in fission of a uranium-like species. The average fission event is a "slow" process with the establishment of statistical equilibrium. Such events are characterized by a modest ($<J>$ ~ 25–35hbar) fissioning system angular momentum and result from a partial transfer of projectile linear momentum to the target nucleus. The trend of increasing fragment anisotropy with decreasing fragment N/Z appears to result from a single mechanism for the initial projectile-target encounter with differing amounts of deposition energy. A small fraction of events are "fast" in character without the establishment of statistical equilibrium. They may be fission-like events (with only the most asymmetric of these events being detected in this study). These unusual events, which have not been observed previously in intermediate energy heavy ion reactions, appear to involve large mass loss (ΔA ~ 50) without disturbing the two-body kinematics of fission. Such events resemble qualitatively, but are crucially different from similar processes observed at lower and higher projectile energies. Comparison of this work with similar studies of Au target fragmentation reveals important differences in the observable outcome of the fragmentation processes in these nuclei of differing fissionability.

ACKNOWLEDGEMENTS

We gratefully acknowledge the assistance of the SC synchrocyclotron operations staff and the CERN health physics staff, and the members of the ISOLDE collaboration. Helpful discussions with C. Gregoire, T. T. Sugihara, and S. B. Kaufman are acknowledged. One of us (PLM) wishes to acknowledge personal support from CERN during the course of the experiment while another of us (WDL) is grateful for the hospitality of the Studsvik Science Research Laboratory during the preparation of this manuscript.

REFERENCES

1 G. D. Harp, J. M. Miller, and B. J. Berne, Phys. Rev. *165*, 1166 (1968).

2 J. B. Cumming, R. J. Cross, Jr., J. Hudis, and A. M. Poskanzer, Phys. Rev. *134*, B167 (1964).

3 R. H. Kraus, Jr., W. Loveland, K. Aleklett, P.L. McGaughey, T. T. Sugihara, G. T. Seaborg, T. Lund, Y. Morita, E. Hagebø, and I. R. Haldorsen, Nucl. Phys. A *432*, 525 (1985).

4 P. L. McGaughey, W. Loveland, D. J. Morrissey, K. Aleklett, and G. T. Seaborg, Phys. Rev. C *31*, 896 (1985). The cross sections for the interaction of 1.O GeV ^{12}C with ^{238}U quoted in this work are too low by a factor of 1.87.

5 M. de Saint-Simon, S. Haan, G. Audi, A. Coe, M. Epherre, P. Guimbal, A. C. Mueller, C. Thibault, and F. Touchard, Phys. Rev. C *26*, 2447 (1982). The relative cross sections measured in this study were reported as absolute values by normalization to unpublished values of cross sections measured by Hagebø and collaborators.

6 U. Lynen, H. Ho, W. Kohn, D. Pelte, U. Winkler, W.F.J. Müller, Y.T. Chu, P. Doll, A. Gobbi, K. Hildenbrand, A. Olmi, H. Sann, H. Stelzer, R. Bock, H. Löhner, R. Glasow, and R. Santo, Nucl. Phys. A *387*, 129c (1982).

7 J. B. Marion, T. I. Arnette, and H. C. Owens, Oak Ridge National Laboratory Report ORNL-2574 (1959).

8 N. T. Porile, S. Pandian, H. Klonk, C. R. Rudy, and E. P. Steinberg, Phys. Rev. C *19*, 1832 (1979).

9 L. Winsberg, Nucl. Instrum. & Meth. *150*, 465 (1978).

10 W. Loveland, K. Aleklett, P. L. McGaughey, K. J. Moody, R. M. McFarland, R. H. Kraus, Jr., and G. T. Seaborg, Lawrence Berkeley Laboratory Report LBL-16280 (November 1983).

11 See, for example, J. Hudis, in *Nuclear Chemistry,* edited by L. Yaffe (Academic, New York, 1968) Vol. 1, p. 169.

12 S. Pandian and N. T. Porile, Phys. Rev. C *23,* 427 (1981).

13 E. M. Friedlander and H. H. Heckman in *Treatise on Heavy Ion Nuclear Science,* edited by D. A. Bromley (Plenum, New York, 1985), Vol. 4, p. 403.

14 W. D. Myers, Nucl. Phys. A *296,* 177 (1978).

15 V. P. Crespo, J. B. Cumming, and A. M. Poskanzer, Phys. Rev. *174,* 1455 (1968).

16 J. R. Huizenga, A. N. Behkami, and L. G. Moretto, Phys. Rev. *177,* 1826 (1969).

17 K. T. Lesko, S. Gil, A. Lazzarini, V. Metag, A. G. Seamster, and R. Vandenbosch, Phys. Rev. C *27,* 2999 (1983)

18 L. Moretto, Nucl. Phys. A *247,* 211 (1975).

19 C. Gregoire, C. Ngô, and B. Remaud, Nucl. Phys. A *383,* 392 (1982). W. W. Wilcke, J. R. Birkelund, H. J. Wollersheim, A. D. Hoover, J. R. Huizenga, W. U. Schröder, and L. E. Tubbs, At. Data and Nucl. Data Tables *25,* 391 (1980).

21 B. D. Wilkins, S. B. Kaufman, E. P. Steinberg, J. A. Urbon, and D. J. Henderson, Phys. Rev. Lett. *43,* 1080 (1979).

22 B. L. Gorshkov, A. I. Iljin, B. Yu. Sokolovsky, G. E. Solyakin, and Yu. A. Chestnov, JETP Letters *37,* 60 (1983).

FIGURE CAPTIONS

FIG. 1. The isobaric yield distribution for the reaction of 85 MeV/nucleon ^{12}C with ^{238}U. From Ref. 4.

FIG. 2. Representative "light" target fragment angular distributions for the interaction of 85 MeV/nucleon ^{12}C with ^{238}U. The solid lines are to guide the eye through the data, the dashed line shows the angular distribution (normalized at 114°) for the same fragment produced in the ^{197}Au (85 MeV/nucleon ^{12}C, X) reaction.

FIG. 3. Representative fission fragment angular distributions for the interaction of 85 MeV/nucleon ^{12}C with ^{238}U. The solid lines are to guide the eye through the data.

FIG. 4. a) Measured angular distributions (normalized at 114°) for the Sb isotopes from the interaction of 85 MeV/nucleon ^{12}C with ^{238}U showing the effect of fragment N/Z upon the distributions. The lines are to guide the eye through the data. The maximum uncertainties in the data are shown. b) Firestreak model calculations of the ^{122}Sb and ^{128}Sb angular distributions.

FIG. 5. Representative "heavy" fragment angular distributions from the interaction of 85 MeV/nucleon ^{12}C with ^{238}U.

FIG. 6. Moving frame angular distributions of V, the kick given the primary target fragment by fission or particle emission for representative "light" fragments. The solid lines are to guide the eye through the data.

FIG. 7. Same as Fig. 6 except the fragments have $84 \leq A \leq 103$. Here the solid lines represent fits to the data using moving frame distributions of the form $W(\theta_{MF}) = \frac{a+b\cos^2\theta}{a+b/3}$.

FIG. 8. Same as Fig. 6 except $139 \leq A \leq 169$. The dashed line for the ^{146}Gd distributions represents the angular distribution expected for the fission fragment complement of ^{46}Sc.

FIG. 9. Portion of isobaric yield distribution for interaction of 84 MeV/nucleon ^{12}C with ^{197}Au showing light fragment and fission fragment yields. The solid line is a possible guide for the eye through the data. From Ref. 10.

Table I

Target Fragment Angular Distributions (mb/sr) for 85 MeV/nucleon $^{12}C + ^{238}U$

Nuclide	7°	20°	32°	44°	57°	71°	114°	133°	151°
^{28}Mg	-	0.39 ± 0.03	0.27 ± 0.06	0.21 ± 0.02	0.14 ± 0.01	0.12 ± 0.01	0.07 ± 0.01	0.05 ± 0.01	0.07 ± 0.01
^{46}Sc	-	0.64 ± 0.13	0.30 ± 0.04	0.19 ± 0.06	0.20 ± 0.03	0.18 ± 0.03	0.16 ± 0.04	0.12 ± 0.01	0.15 ± 0.02
^{48}Sc	-	0.34 ± 0.05	0.28 ± 0.02	0.26 ± 0.01	.20 ± 0.02	0.21 ± 0.03	0.16 ± 0.03	0.16 ± 0.02	0.15 ± 0.04
^{59}Fe	-	1.08 ± 0.04	1.07 ± 0.03	0.87 ± 0.03	0.70 ± 0.04	0.71 ± 0.02	0.59 ± 0.02	0.54 ± 0.04	0.52 ± 0.02
^{74}As	1.63 ± 0.33	1.17 ± 0.11	1.09 ± 0.08	0.95 ± 0.05	0.81 ± 0.03	0.70 ± 0.05	0.63 ± 0.02	0.59 ± 0.03	0.55 ± 0.03
^{75}Se	-	0.73 ± 0.13	0.62 ± 0.07	0.60 ± 0.08	0.52 ± 0.06	0.42 ± 0.06	0.35 ± 0.00	0.37 ± 0.02	0.33 ± 0.05
^{83}Rb	-	2.02 ± 0.10	1.91 ± 0.08	1.70 ± 0.05	1.41 ± 0.09	1.22 ± 0.03	1.04 ± 0.05	0.99 ± 0.04	1.00 ± 0.05
^{84}Rb	-	2.91 ± 0.20	2.62 ± 0.21	2.47 ± 0.20	1.98 ± 0.05	1.68 ± 0.05	1.48 ± 0.02	1.40 ± 0.08	1.37 ± 0.08
^{87}Y	2.43 ± 0.39	2.01 ± 0.12	1.91 ± 0.10	1.61 ± 0.15	1.37 ± 0.09	1.11 ± 0.11	0.90 ± 0.08	0.90 ± 0.15	0.87 ± 0.07
^{88}Y	3.14 ± 0.29	2.49 ± 0.10	2.28 ± 0.15	2.06 ± 0.11	1.67 ± 0.05	1.47 ± 0.08	1.22 ± 0.09	1 24 ± 0.03	1.17 ± 0.04
^{89}Zr	2.77 ± 0.18	1.46 ± 0.08	1.42 ± 0.07	1.20 ± 0.07	1.01 ± 0.05	0.82 ± 0.04	0.70 ± 0.04	0.70 ± 0.04	0.65 ± 0.05
*^{91}Sr	-	1.18 ± 0.23	1.22 ± 0.16	1.24 ± 0.06	1.08 ± 0.03	1.01 ± 0.20	0.97 ± 0.11	0.94 ± 0.06	0.99 ± 0.05
^{95}Zr	5.65 ± 1.21	6.50 ± 0.21	6.28 ± 0.26	5.91 ± 0.42	5.28 ± 0.16	5.07 ± 0.21	5.12 ± 0.11	4.86 ± 0.11	4.70 ± 0.37
^{97}Zr	3.64 ± 0.72	4.11 ± 0.40	4.40 ± 0.50	3.93 ± 0.54	3.72 ± 0.36	3.64 ± 0.43	3.50 ± 0.29	3.25 ± 0.25	3.43 ± 0.25
^{97}Ru	0.55 ± 0.06	0.44 ± 0.02	0.44 ± 0.04	0.36 ± 0.02	0.31 ± 0.02	0.25 ± 0.04	0.19 ± 0.04	0.21 ± 0.03	0.20 ± 0.03
^{99}Mo	6.45 ± 0.19	6.35 ± 0.24	6.21 ± 0.29	5.82 ± 0.29	5.34 ± 0.34	4.76 ± 0.19	4.67 ± 0.19	4.57 ± 0.24	4.67 ± 0.24
$^{101}Rh^m$	-	1.12 ± 0.24	1.07 ± 0.19	0.94 ± 0.12	0.79 ± 0.04	0.63 ± 0.17	0.48 ± 0.05	0.49 ± 0.05	0.46 ± 0.09
^{103}Ru	11.6 ± 1.13	11.4 ± 0.4	10.0 ± 1.0	9.8 ± 0.6	9.4 ± 0.4	8.3 ± 0.3	8.2 ± 0.3	8.0 ± 0.3	7.8 ± 0.3
^{105}Rh	-	10.5 ± 0.6	10.4 ± 0.4	9.3 ± 0.4	8.4 ± 0.3	7.4 ± 0.2	6.9 ± 0.4	7.3 ± 1.0	7.0 ± 0.3
*^{105}Ag	-	2.32 ± 0.22	2.14 ± 0.22	1.80 ± 0.54	1.52 ± 0.10	1.26 ± 0.15	0.97 ± 0.17	1.09 ± 0.12	-
$^{106}Ag^m$	1.13 ± 0.19	1.02 ± 0.17	1.05 ± 0.16	0.88 ± 0.07	0.82 ± 0.07	0.61 ± 0.03	0.50 ± 0.05	0.48 ± 0.03	0.46 ± 0.02
$^{110}Ag^m$	-	2.60 ± 0.47	2.46 ± 0.14	2.14 ± 0.06	1.81 ± 0.10	1.47 ± 0.04	1.34 ± 0.03	1.36 ± 0.10	1.34 ± 0.17
^{111}In	1.54 ± 0.2	1.40 ± 0.05	1.26 ± 0.10	1.13 ± 0.10	0.96 ± 0.08	0.73 ± 0.03	0.56 ± 0.08	0.58 ± 0.03	0.54 ± 0.06
*^{112}Pd	-	1.29 ± 0.11	1.08 ± 0.16	1.10 ± 0.13	1.05 ± 0.14	0.93 ± 0.04	0.97 ± 0.06	0.93 ± 0.08	0.97 ± 0.05
$^{114}In^m$	-	2.02 ± 0.21	2.00 ± 0.07	1.87 ± 0.15	1.62 ± 0.11	1.26 ± 0.11	1.15 ± 0.07	1.15 ± 0.09	1.10 ± 0.04
^{115}Cd	3.08 ± 0.44	3.83 ± 0.44	3.66 ± 0.14	3.52 ± 0.17	3.28 ± 0.22	2.70 ± 0.17	2.67 ± 0.17	2.92 ± 0.25	2.83 ± 0.14
$^{117}Sn^m$	-	2.74 ± 0.52	2.42 ± 0.41	2.22 ± 0.25	1.93 ± 0.29	1.50 ± 0.24	1.29 ± 0.16	1.33 ± 0.19	1.33 ± 0.03
$^{119}Te^m$	1.36 ± 0.05	1.26 ± 0.07	1.27 ± 0.04	1.08 ± 0.08	0.90 ± 0.06	0.66 ± 0.03	0.52 ± 0.03	0.59 ± 0.01	0.53 ± 0.04
$^{120}Sb^m$	1.96 ± 0.24	2.00 ± 0.17	1.78 ± 0.17	1.56 ± 0.12	1.34 ± 0.04	1.02 ± 0.04	0.87 ± 0.02	0.96 ± 0.04	0.91 ± 0.04
$^{121}Te^m$	-	1.71 ± 0.04	1.71 ± 0.09	1.47 ± 0.03	1.26 ± 0.03	0.93 ± 0.06	0.82 ± 0.02	0.85 ± 0.03	0.78 ± 0.03
^{122}Sb	-	2.11 ± 0.23	2.07 ± 0.06	1.80 ± 0.06	1.60 ± 0.04	1.25 ± 0.02	1.17 ± 0.02	1.25 ± 0.07	1.25 ± 0.05
^{124}Sb	2.08 ± 0.44	1.84 ± 0.10	1.84 ± 0.01	1.83 ± 0.10	1.55 ± 0.14	1.28 ± 0.05	1.32 ± 0.10	1.32 ± 0.12	1.20 ± 0.11
^{124}I	2.28 ± 0.24	1.61 ± 0.31	1.59 ± 0.26	1.53 ± 0.08	1.33 ± 0.09	1.03 ± 0.10	0.93 ± 0.10	1.01 ± 0.34	0.96 ± 0.27
^{126}Sb	0.98 ± 0.26	1.07 ± 0.26	1.19 ± 0.17	1.12 ± 0.15	1.05 ± .13	0.86 ± 0.18	0.88 ± 0.08	0.93 ± 0.13	0.87 ± 0.22
*^{128}Sb	-	0.98 ± 0.30	1.12 ± 0.21	1.00 ± 0.18	1.15 ± 0.30	1.03 ± 0.28	0.97 ± 0.10	0.98 ± 0.05	1.02 ± 0.13
^{131}I	3.17 ± 0.43	2.90 ± 0.19	2.93 ± 0.14	2.93 ± 0.05	2.77 ± 0.08	2.39 ± 0.05	2.63 ± 0.08	2.58 ± 0.08	2.50 ± 0.08
^{132}Te	1.56 ± 0.07	1.66 ± 0.13	1.69 ± 0.14	1.52 ± 0.10	1.52 ± 0.01	1.31 ± 0.01	1.35 ± 0.06	1.36 ± 0.01	1.38 ± 0.06
*^{133}I	-	1.13 ± 0.08	1.12 ± 0.09	1.15 ± 0.06	0.96 ± 0.02	0.92 ± 0.04	0.97 ± 0.06	0.99 ± 0.03	0.95 ± 0.12
*^{133m}Ba	-	1.35 ± 0.42	1.45 ± 0.26	1.25 ± 0.13	1.18 ± 0.10	0.92 ± 0.07	0.97 ± 0.15	0.91 ± 0.14	0.93 ± 0.10
^{136}Cs	-	0.86 ± 0.08	0.89 ± 0.10	0.87 ± 0.07	0.78 ± 0.06	0.61 ± 0.04	0.67 ± 0.02	0.70 ± 0.08	0.65 ± 0.04
^{139}Ce	-	3.14 ± 0.14	2.87 ± 0.09	2.41 ± 0.16	1.96 ± 0.10	1.30 ± 0.07	1.01 ± 0.08	1.19 ± 0.08	1.04 ± 0.05
^{140}Ba	1.29 ± 0.15	1.57 ± 0.10	1.57 ± 0.08	1.64 ± 0.04	1.54 ± 0.05	1.28 ± 0.03	1.33 ± 0.04	1.40 ± 0.11	1.35 ± 0.07
^{143}Ce	-	1.59 ± 0.10	1.78 ± 0.20	1.82 ± 0.06	1.71 ± 0.01	1.31 ± 0.06	1.38 ± 0.07	1.57 ± 0.16	1.41 ± 0.10
*^{146}Gd	15.0 ± 1.8	11.80 ± 0.70	8.42 ± 0.42	5.87 ± 0.33	3.85 ± 0.21	1.95 ± 0.26	0.97 ± 0.06	1.01 ± 0.16	0.99 ± 0.09
^{149}Gd	-	1.19 ± 0.13	0.86 ± 0.17	0.74 ± 0.22	-	-	0.16 ± 0.06	-	-
*^{153}Gd	-	4.10 ± 1.00	3.50 ± 1.20	3.60 ± 1.00	2.03 ± 0.32	1.08 ± 0.45	0.97 ± 0.53	0.96 ± 0.06	0.89 ± 0.44
^{169}Yb	-	1.52 ± 0.11	1.16 ± 0.10	0.86 ± 0.17	0.43 ± 0.08	0.18 ± 0.02	0.08 ± 0.01	-	-
*^{185}Os	-	26.40	18.0	9.40	4.10	1.60	0.97	0.88	-

* Denotes cross section in arbitrary units, not mb/sr.

Table II
Deduced Fragment Characteristics
85 MeV/nucleon $^{12}C + ^{238}U$

Fragment	$\eta_{parallel}$	b/a	Fragment	$\eta_{parallel}$	b/a
^{28}Mg	0.418	-	$^{114}In^{m}$	0.140	0.36
^{46}Sc	0.266	-	^{115}Cd	0.0656	0.15
^{48}Sc	0.209	-	$^{117}Sn^{m}$	0.170	0.51
^{59}Fe	0.166	-	$^{119}Te^{m}$	0.236	0.7
^{74}As	0.175	-	$^{120}Sb^{m}$	0.175	0.64
^{75}Se	0.159	0.67	$^{121}Te^{m}$	0.183	0.5
^{83}Rb	0.176	0.41	^{122}Sb	0.131	0.40
^{84}Rb	0.179	0.38	^{124}Sb	0.111	0.18
^{87}Y	0.220	0.55	^{124}I	0.159	0.50
^{88}Y	0.189	0.67	^{126}Sb	0.0567	0.15
^{89}Zr	0.191	0.50	^{128}Sb	0.0226	0.05
^{91}Sr	0.0427	0.10	^{131}I	0.0308	0.11
^{95}Zr	0.0469	0.17	^{132}Te	0.0266	0.27
^{97}Zr	0.0496	0.10	^{133}I	0.0281	0.10
^{97}Ru	0.225	0.74	$^{133}Ba^{m}$	0.109	0.30
^{99}Mo	0.0532	0.25	^{136}Cs	0.0729	0.0729
$^{101}Rh^{m}$	0.229	0.6	$^{139}C3$	0.299	-
^{103}Ru	0.0690	0.23	^{140}Ba	0.0459	0.0459
^{105}Rh	0.0851	0.27	^{143}Ce	0.0591	0.13
^{105}Ag	0.217	0.7	^{146}Gd	0.637	-
$^{106}Ag^{m}$	0.215	0.45	^{149}Gd	0.514	-
$^{110}Ag^{m}$	0.139	0.5	^{153}Gd	0.379	-
^{111}In	0.227	0.78	^{169}Yb	0.736	-
^{112}Pd	0.0405	0.15	^{185}Os	0.764	-

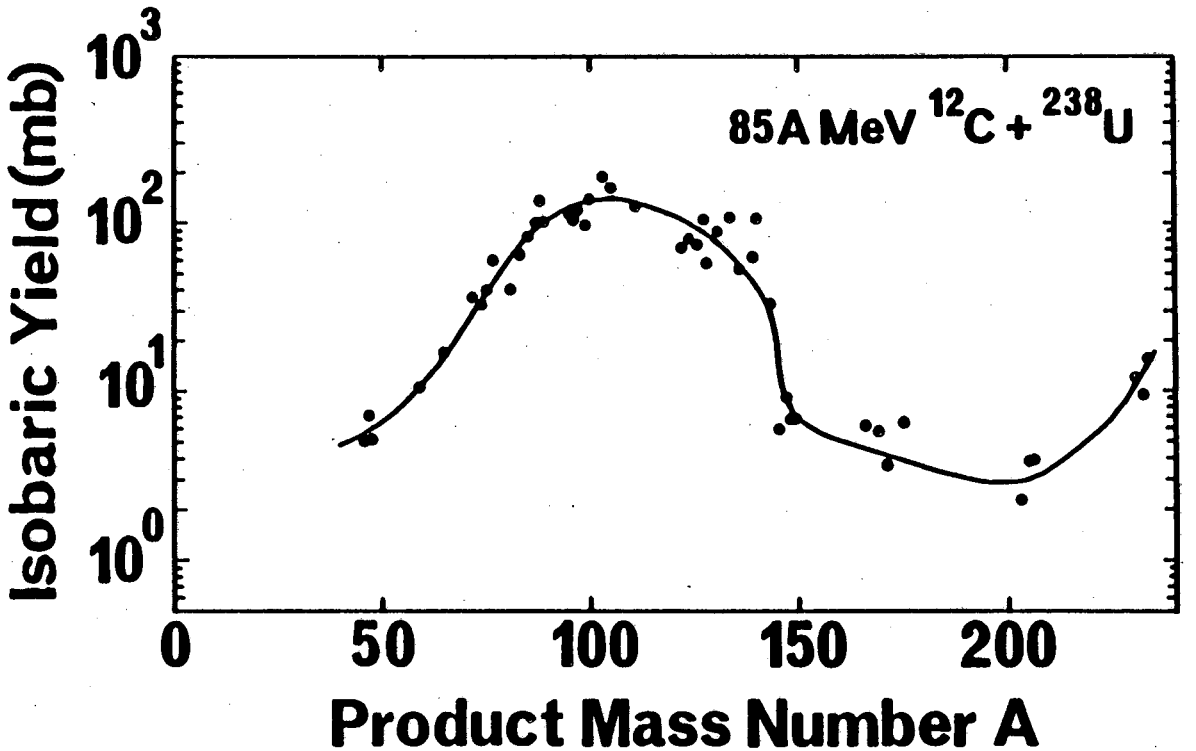
85A MeV $^{12}C + ^{238}U$
Isobaric Yield (mb)
10^3
10^2
10^1
10^0
0
50
100
150
200
Product Mass Number A

Fig. 1

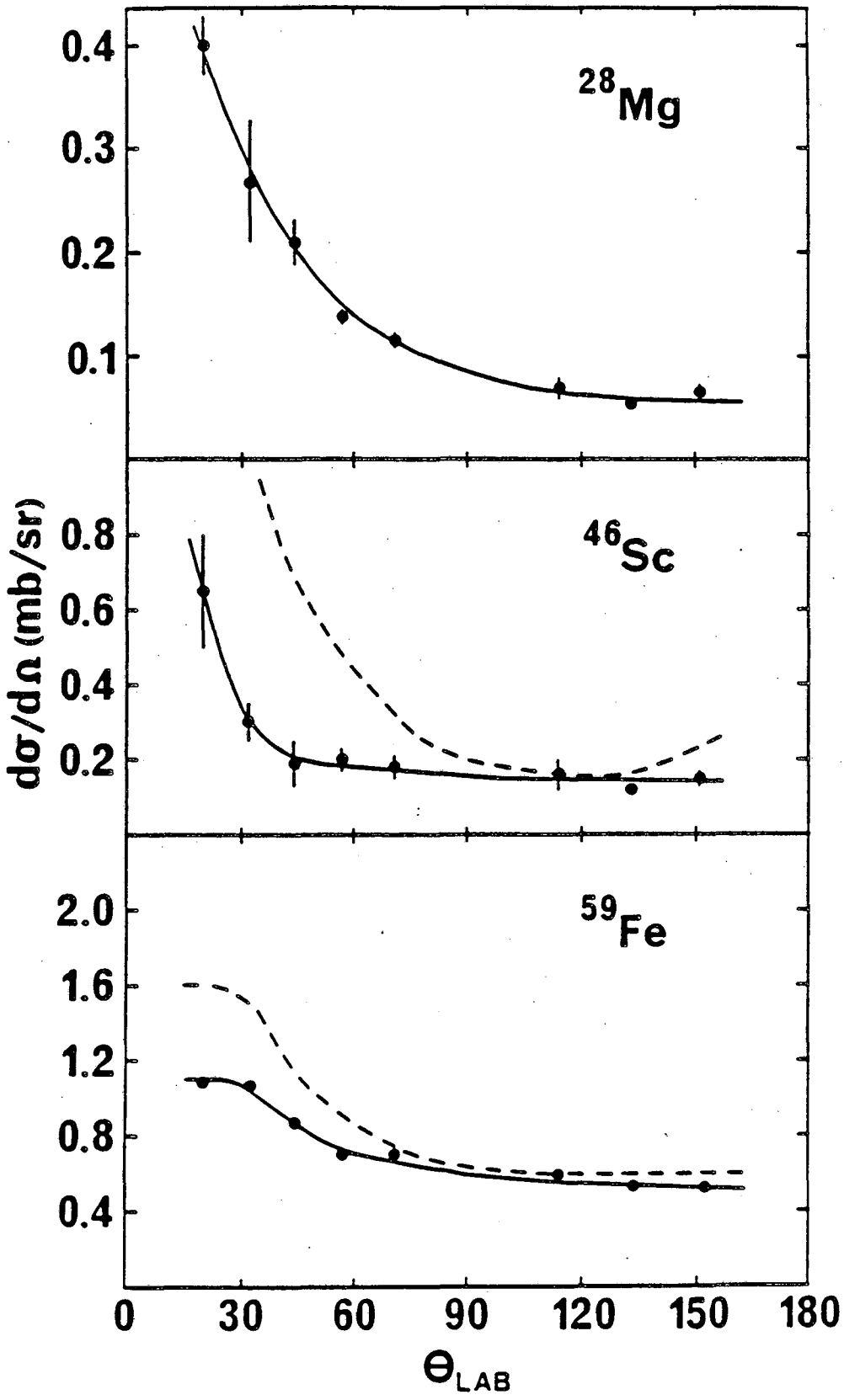
0.4
0.3
0.2
0.1
^{28}Mg
0.8
0.6
0.4
0.2
^{46}Sc
dσ/dΩ (mb/sr)
2.0
1.6
1.2
0.8
0.4
^{59}Fe
0
30
60
90
120
150
180
θ_{LAB}

Fig. 2

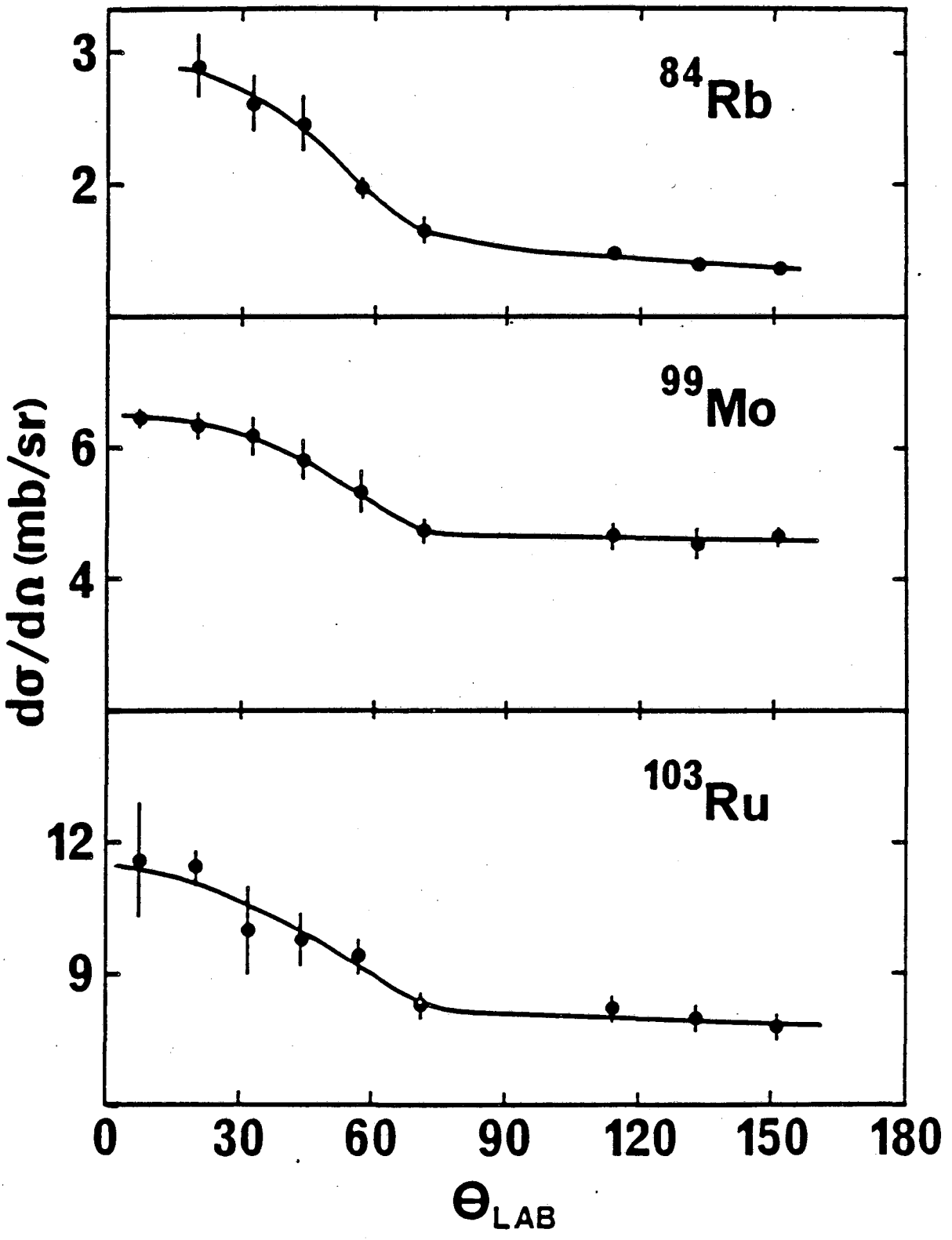
3
2
^{84}Rb
6
4
^{99}Mo
12
9
^{103}Ru
dσ/dΩ (mb/sr)
0
30
60
90
120
150
180
Θ_{LAB}

Fig. 3

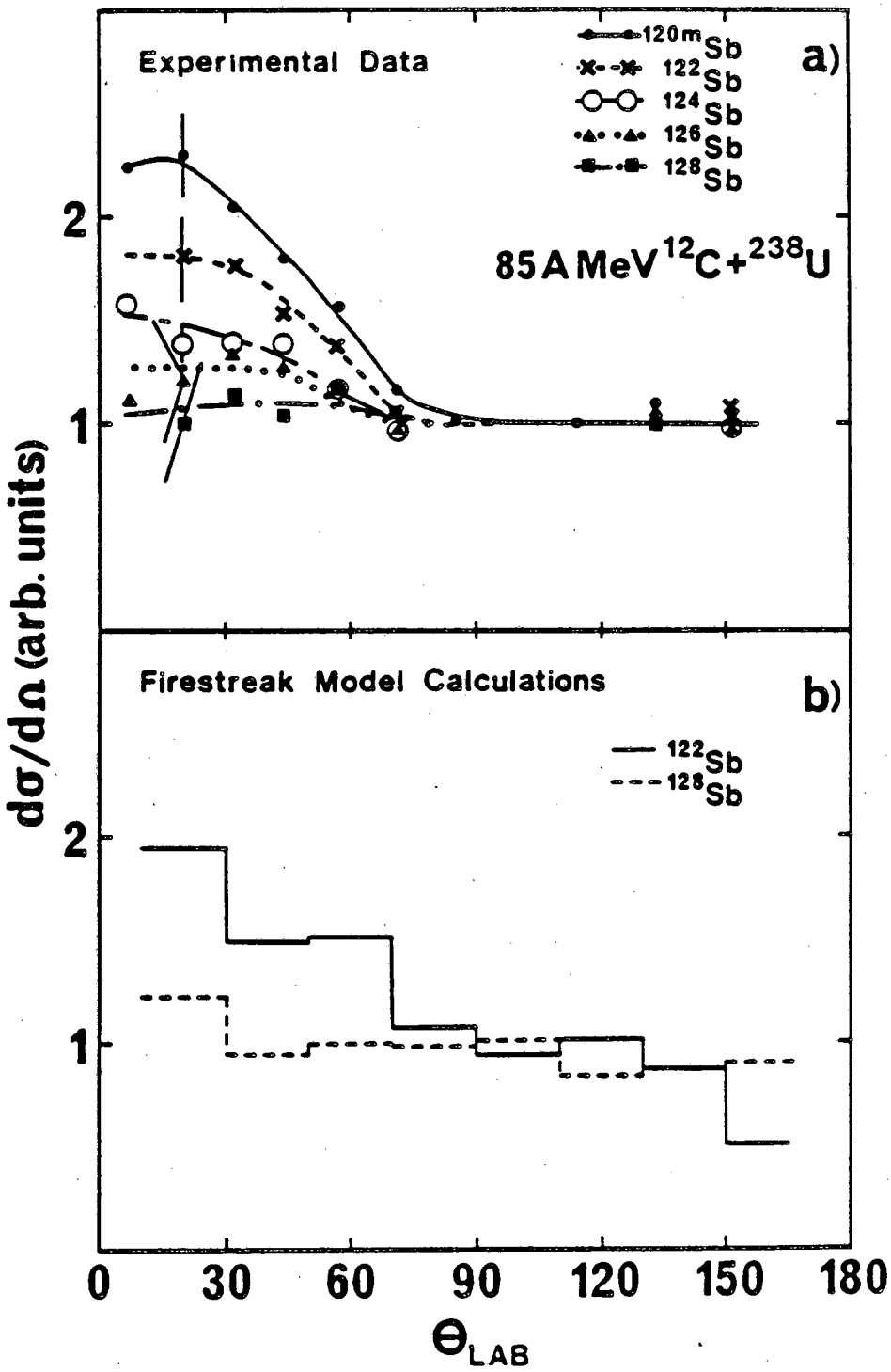
Experimental Data
a)
120m Sb
122 Sb
124 Sb
126 Sb
128 Sb
85 A MeV 12C+238U
Firestreak Model Calculations
b)
122 Sb
128 Sb
dσ/dΩ (arb. units)
2
1
0
30
60
90
120
150
180
ΘLAB

Fig. 4

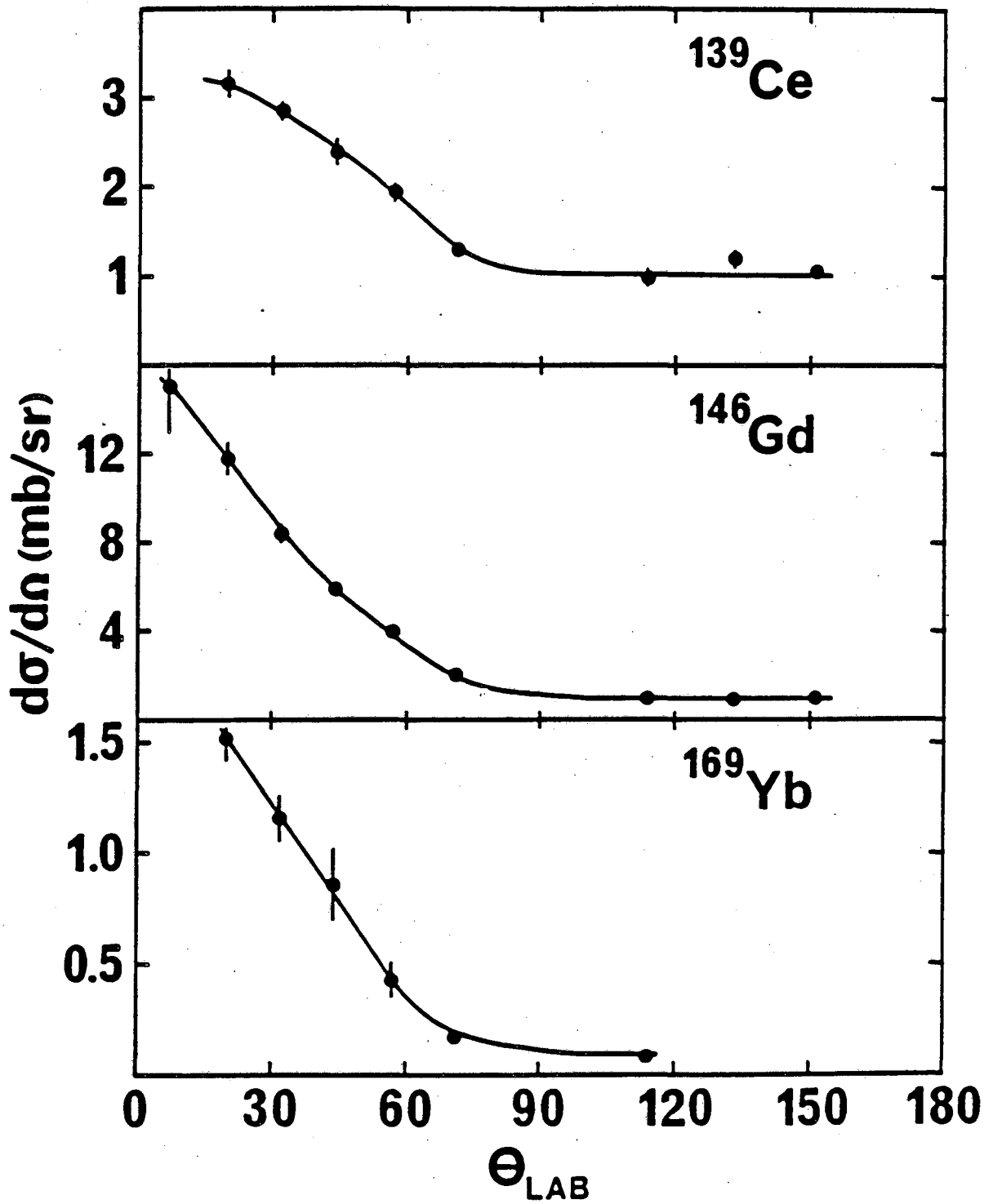
139Ce
146Gd
169Yb
dσ/dΩ (mb/sr)
3
2
1
12
8
4
1.5
1.0
0.5
0
30
60
90
120
150
180
θLAB

Fig. 5

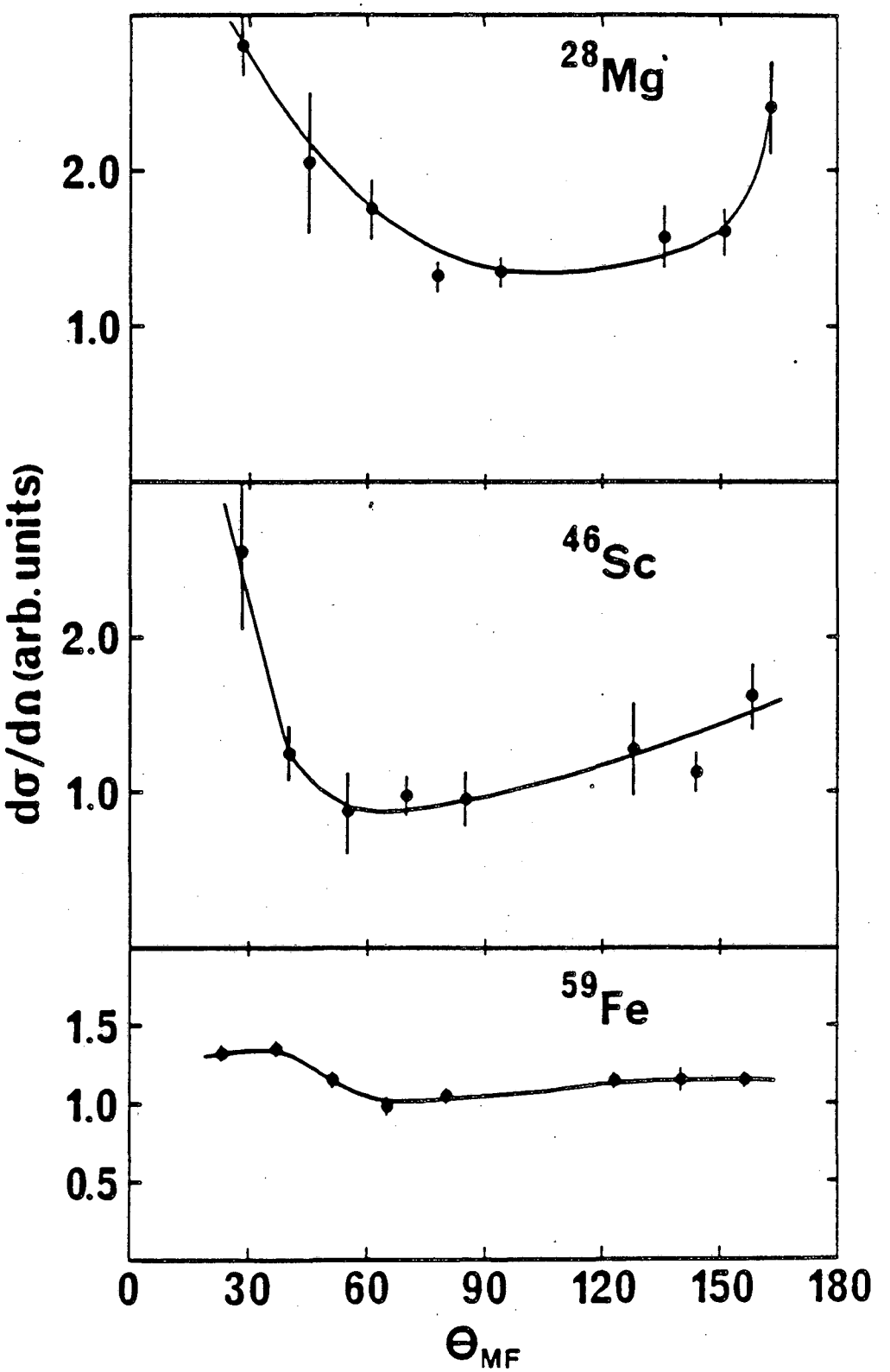
^{28}Mg
^{46}Sc
^{59}Fe
2.0
1.0
2.0
1.0
1.5
1.0
0.5
dσ/dΩ (arb. units)
0
30
60
90
120
150
180
Θ_{MF}

Fig. 6

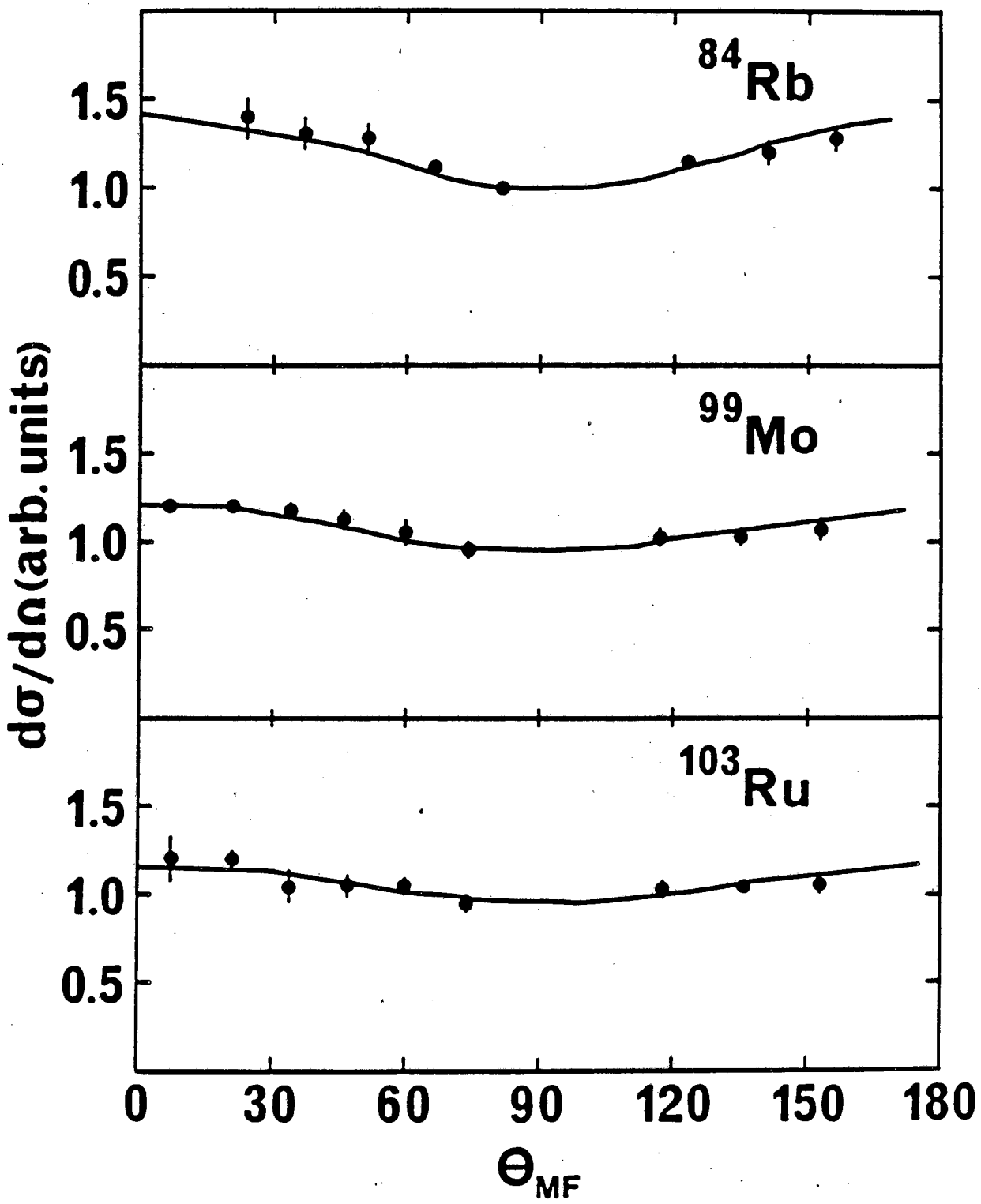
^{84}Rb
^{99}Mo
^{103}Ru
1.5
1.0
0.5
dσ/dΩ(arb. units)
0
30
60
90
120
150
180
Θ_{MF}

Fig. 7

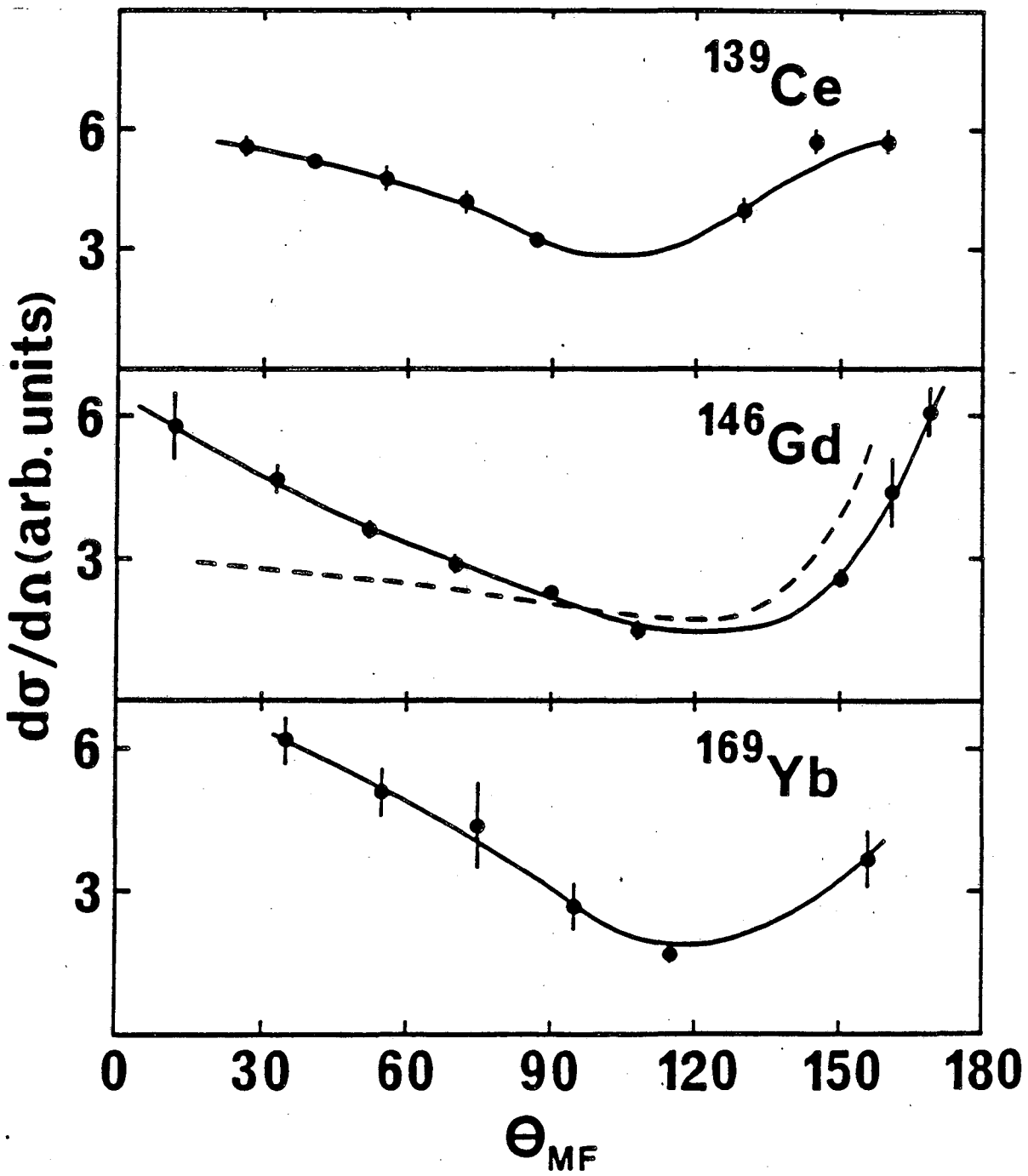

Fig. 8

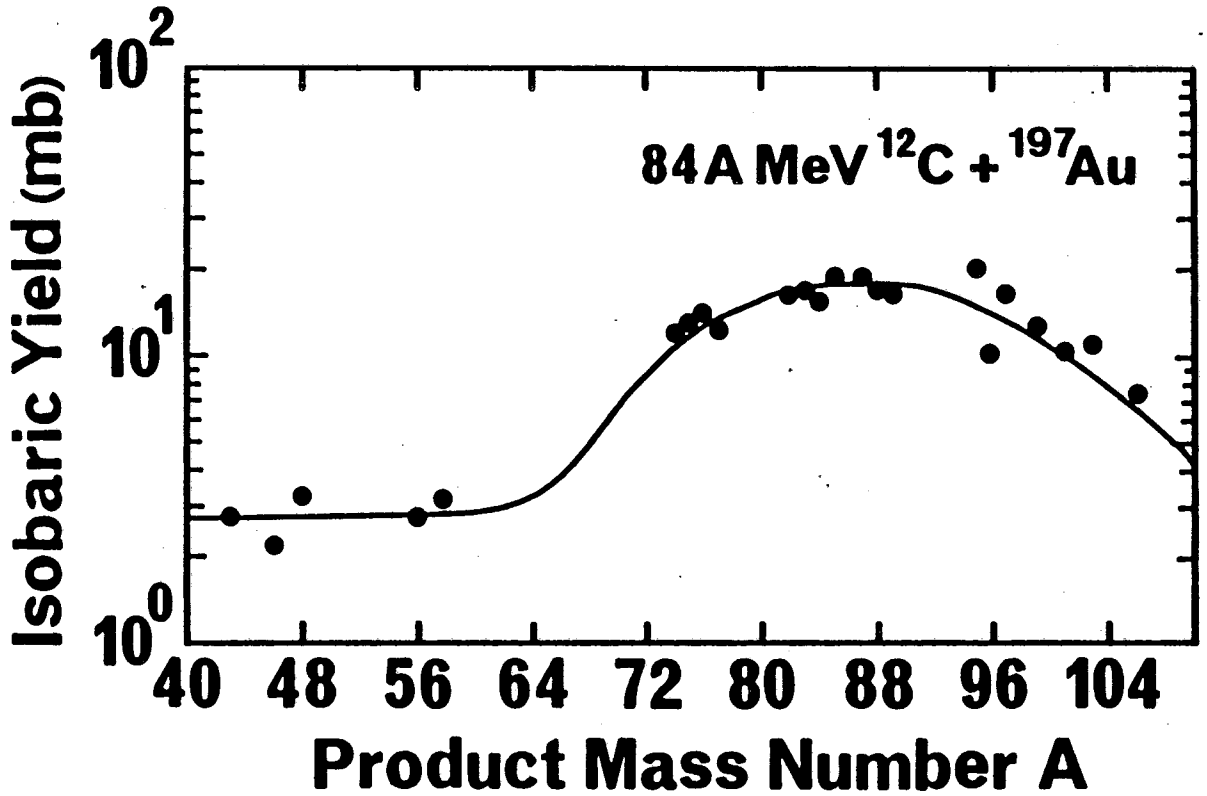
84 A MeV ^{12}C + ^{197}Au
Isobaric Yield (mb)
10^2
10^1
10^0
40 48 56 64 72 80 88 96 104
Product Mass Number A

Fig. 9

This report was done with support from the Department of Energy. Any conclusions or opinions expressed in this report represent solely those of the author(s) and not necessarily those of The Regents of the University of California, the Lawrence Berkeley Laboratory or the Department of Energy.

Reference to a company or product name does not imply approval or recommendation of the product by the University of California or the U.S. Department of Energy to the exclusion of others that may be suitable.

LAWRENCE BERKELEY LABORATORY
TECHNICAL INFORMATION DEPARTMENT
UNIVERSITY OF CALIFORNIA
BERKELEY, CALIFORNIA 94720